Construction and Building Materials 411 (2024) 134424

Contents lists available at ScienceDirect

Construction and Building Materials

journal homepage: www.elsevier.com/locate/conbuildmat

Size effect on the flexural fatigue behavior of high-strength plain and fiber-reinforced concrete

Álvaro Mena-Alonso *, Dorys C. González, Jesús Mínguez, Miguel A. Vicente

Department of Civil Engineering, University of Burgos, C/ Villadiego s/n, 09001 Burgos, Spain

ARTICLE INFO

Keywords:
Size effect
Flexural fatigue
Fiber-reinforced concrete
Cracking in concrete
Secondary crack opening rate

ABSTRACT

This paper studies the size effect on flexural fatigue in concrete. In particular, the main objective is to evaluate how the addition and content of steel fibers affect this size effect. For this purpose, four types of concrete have been produced: plain and reinforced concrete with fiber contents of 0.3%, 0.6% and 1%. Two prismatic specimen sizes were considered: 75×75×300 mm, named S, and 150×150×600 mm, named L. All specimens were subjected to 3-point bending fatigue at the same relative stress levels up to failure. The results reveal very interesting conclusions. The fibers mitigate the size effect on fatigue life, going from a difference of three orders of magnitude in PC, to practically zero in SFRC. Furthermore, it is observed that fibers do not necessarily improve fatigue life; in fact, the trend changes depending on specimen size. Finally, it is shown that the secondary crack opening rate dCMOD/dn has a good correlation with fatigue life, explaining the dispersion of N in general and the size effect in particular.

1. Introduction

Fatigue in concrete is a complex phenomenon, since it implies that a given element can fail without even having exceeded its ultimate load under static conditions. This type of action is gaining relevance in recent years, since, with the development of high strength concretes, structures are becoming increasingly slender. As a result, the importance of variable loads (traffic, wind, etc.), cyclic in nature and responsible for fatigue, is increasing.

There is one issue related to fatigue in concrete that has not yet been satisfactorily resolved. This is the size effect; that is, the reduction of mechanical strength in geometrically similar elements with increasing size. This problem is not exclusive to fatigue but is observed in the structural response of concrete in general (compressive strength, flexural strength, etc.). In the particular case of fatigue, this means that if two homothetic specimens of different sizes are subjected to cyclic loading under the same stress levels, the resulting fatigue life is expected to be greater in the smaller specimens.

The study of the size effect is of great interest, since normally the experimental determination of concrete strength (fatigue strength, compressive strength, etc.) is made on specimens that are several orders of magnitude smaller than the real elements. Therefore, if the results are not properly corrected, an overestimation of the concrete capacity may be incurred, with the consequent risk to structural safety.

This lack of understanding of the size effect, together with the large scatter that fatigue results usually show, makes the safety margins in fatigue design very conservative. For example, according to Eurocode 2 [1], in concrete with a characteristic compressive strength f_{ck} of 80 MPa, its design fatigue strength $f_{cd,fat}$ is only 36 MPa [2]. Consequently, it is necessary to advance in the knowledge of these phenomena, so that it is possible to reduce the safety coefficients and optimize the strength of concrete. This is critical for structures whose design is conditioned by fatigue, such as concrete wind turbine towers.

There are different causes that explain the size effect on the mechanical strength of concrete. The most accepted theory at present is the size effect law in quasi-brittle materials (SEL) developed by Bažant [3]. This theory is based on the crack growth process in concrete; more specifically, on the fracture process zone (FPZ), an area of microcracks with a certain cohesive capacity that is generated at the crack front. It is observed that the proportion of energy released in the FPZ for a certain increment of crack length varies as a function of element size. The practical consequence is that small specimens are more ductile and large specimens are more brittle. Considering the strength-size curve in concrete structures (Fig. 1) [3,4], this means that small elements approach a plastic analysis by strength criteria, independent of size. On the contrary, in large elements, the linear elastic fracture mechanics (LEFM)

* Corresponding author.
E-mail address: amena@ubu.es (Á. Mena-Alonso).

https://doi.org/10.1016/j.conbuildmat.2023.134424

Available online 8 December 2023

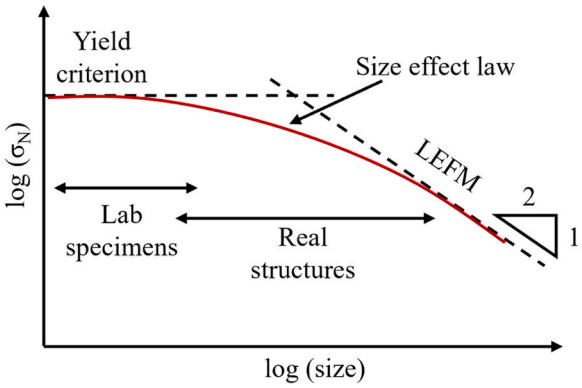

Fig. 1. Strength-size curve in concrete structures
Adapted from [5].

Fig. 2. Examples of real specimens of size S and L already tested.

theory, typical of brittle materials and characterized by a strong size effect, would be applicable. The actual behavior of concrete in the usual size range is a transition between these two extreme behaviors, which means that it is ultimately affected by a certain size effect.

Fracture mechanics of concrete partially explains the size effect, but there are more physical phenomena that cause it. Among them is the wall effect, which is due to the concrete layer in contact with the wall of the mold or formwork having different properties from those inside the element. The size effect occurs because the thickness of the surface layer is independent of the size of the elements, which means that in small specimens it occupies a large proportion of the cross-section compared to large specimens.

In plain concrete (PC), the contribution of the wall effect to the size effect is not very significant [4]. However, in steel fiber-reinforced concrete (SFRC) it plays an essential role since it conditions the position and orientation of the fibers. Under bending, fibers determine the concrete behavior after cracking, and even the ultimate strength if strain-hardening occurs when certain conditions are met. The higher the ratio between the fiber length and the minimum dimension of the element, the more aggressive the wall effect will be, causing the fibers to tend to align in the direction of the largest specimen dimension, and ultimately resulting in better flexural behavior. This is one of the reasons why flexural testing standards set a maximum fiber length / minimum mold dimension ratio, which is usually around 0.3–0.4 [6,7].

Size effect in concrete subjected to flexural stress is a well-known phenomenon [3,4], although in the particular case of SFRC experimental works are not very abundant [8–13]. This is explained because the development of fracture mechanics in SFRC is still low compared to that of PC [14–16]. Li et al. [8] observed that the incorporation of fibers reduces the structural size effect of concrete, shifting the size range in which the transition of brittle-ductile behaviors occurs. In this way, when ductile failure is reached due to sufficient fiber bridging, the nominal stress depends mainly on the fibers and the properties of the fiber-matrix interface. Yoo et al. [12] studied size effect in SFRC of normal and high strengths, considering different fiber contents and types (hooked-end and amorphous). The results showed that high strength concrete is more sensitive to the size effect on flexural strength than normal concrete. Moreover, size effect decreased with increasing fiber volume, being more effective the addition of fibers in high-strength concrete than in normal concrete, which is explained by better fiber-matrix adhesion. In another work by the same author [11], it was observed that a higher fiber slenderness reduced the size effect of SFRC, having a higher yield and providing more ductility. Likewise, it was determined that a possible explanation for size effect is the worse orientation of the fibers in the larger specimens.

Regarding the size effect under cyclic loading, publications are scarce and most of them deal with flexural fatigue in plain concrete [17–23]. One of the most remarkable works is that of Bažant & Xu [19], who were the first to propose the application of the Paris law to the study of the size effect in fatigue; for this purpose, they combined it with the size effect law for quasi-brittle materials under monotonic loading, previously developed by Bažant [3].

With respect to SFRC, works are very scarce, particularly in flexural fatigue [24]. In compressive fatigue, most of the papers are on experimental campaigns [25–28]. Ortega et al. [26] analyzed the size effect on the compressive fatigue behavior of cubic specimens of three sizes, containing 0.3% of steel fibers. A clear size effect on fatigue life was observed, attributed to differences in the stress states of the specimens as a result of the different relationship between the macroscopic size of the specimen and the mesoscopic size of the internal concrete structure. In a later study with the same type of concrete, but this time with cylindrical specimens of the same slenderness, González et al. [25] also observed a marked size effect, proposing different causes to explain it, such as the statistical distribution of larger pores or the maturation or improvement of the compressive strength induced by cyclic loading.

This paper has been developed from the results of [29]. The objective of this work is to experimentally study the size effect in flexural fatigue of plain and steel fiber-reinforced concrete. For this purpose, fatigue tests have been performed on two specimen sizes, working with four different concrete dosages (PC and SFRC with fiber contents of 0.3%, 0.6% and 1%). All tests have been performed under the same relative stress levels (in relation to the average ultimate flexural strength of each type of concrete and specimen size). In this way, it is sought to determine whether the size effect in fatigue varies with the presence of fibers and their dosage.

The article is structured as follows. Section 2 deals with the experimental program, including the description of the specimens and types of concrete tested (2.1), the static characterization of the concrete (2.2) and the description of the fatigue tests (2.3). Then, Section 3 presents the results and discussion, with emphasis on the fatigue behavior. Finally, Section 4 summarizes the main conclusions.

2. Experimental program

2.1. Specimens and types of concrete

In this size effect study, two prismatic specimen sizes have been considered: one with dimensions of 75×75×300 mm, called S, and another of 150×150×600 mm, called L. The latter coincides with the standard specimen size for the determination of flexural strength in fiber-reinforced concrete (EN 14651 [7]). The dimensions of the S-type specimens are half those of the L-type specimens, so that the volume scale factor is 1/8. Fig. 2 shows an image comparing the two specimen sizes.

Although the work focuses exclusively on two specimen sizes, it should be emphasized that 4 types of concrete have been studied: plain concrete (PC) and fiber-reinforced concrete (SFRC) with 3 different fiber contents. Moreover, all the concretes produced are of high strength and

Table 1
Concrete mixtures.

Component	A0	A1	A2	A3
Cement (kg/m3)	400.0			
Coarse aggregate (kg/m3)	538.2			
Fine aggregate (kg/m3)	847.1			
Filler (kg/m3)	448.8			
Water (kg/m3)	160.0			
Superplasticizer (kg/m3)	16.0			
Nanosilica (kg/m3)	20.0			
Steel fibers (kg/m3)	0.0	23.6	47.1	78.5
w/c ratio	0.4			
Steel fibers (% vol.)	0.0%	0.3%	0.6%	1.0%

Table 2
Average results of slump flow test (standard deviation in parentheses).

Concrete type	d_f (mm)	t_{50} (s)
A0	843 (13)	4.8 (0.5)
A1	768 (13)	5.1 (0.5)
A2	739 (37)	4.9 (0.4)
A3	648 (44)	5.5 (0.4)

self-compacting.

The design of the dosages was carried out so that the only difference between the 4 concretes was the fiber content. Portland cement CEM I 52.5 R was used. The aggregates used were silica sand of fraction 0/4 and silica gravel 4/10. In addition, limestone filler of size less than 63 μm was added. Two additives were used. On the one hand, MasterRoc MS 685 (BASF, Ludwigshafen am Rhein, Germany), a nanosilica suspension indicated to improve workability and prevent water migration. On the other hand, MasterEase 5025 superplasticizer, also manufactured by BASF, which provides very liquid consistencies while maintaining relatively low w/c ratios.

Regarding the fibers, Dramix RC-80/30-CP steel fibers (Bekaert, Zwevegem, Belgium) were used. These are 30 mm long hooked-end fibers with an aspect ratio of 78.9. The fiber contents of the 3 SFRC types are 0.3% (low), 0.6% (medium) and 1% (high). The lowest dosage corresponds approximately to the minimum recommended by the manufacturer.

Table 1 contains the dosages of the 4 types of concrete. Type A0 is plain concrete, while types A1 to A3 are SFRC.

For each type of concrete, 16 prismatic specimens L and 16 prismatic specimens S were manufactured. Thus, the size effect study consisted of 8 series of specimens: 4 of size L (A0-L, A1-L, A2-L and A3-L) and 4 of size S (A0-S, A1-S, A2-S and A3-S). The pairs of series corresponding to the same type of concrete (A0-L and A0-S, A1-L and A1-S, A2-L and A2-S, A3-L and A3-S) were produced together. In addition, 8 cylindrical specimens of 150 × 300 mm were casted in each case. Due to the high volume of material, four concrete batches were required for each type of concrete.

All specimens were kept in a climatic chamber at 20 °C and 95% humidity for 1 year. After that, they remained in laboratory conditions for a further 4 months. The reason is to avoid that the gain of strength of the concrete with time introduces uncertainty in the fatigue results. After more than 1 year, it can be assumed that the concrete strength remains approximately constant, at least for the duration of the experimental campaign.

2.2. Concrete characterization

Prior to the fatigue tests, the four types of concrete were characterized. In particular, slump flow tests were performed on fresh concrete, as well as compressive strength and modulus of elasticity tests on hardened concrete. In addition, to determine the static response depending on the type of concrete and the specimen size, three-point bending tests were performed on the eight series of prismatic specimens.

Table 3
Mean compressive strength (standard deviation in parentheses).

Concrete type	f_c (MPa)
A0	107.1 (1.7)
A1	106.6 (3.4)
A2	106.2 (2.0)
A3	107.2 (1.3)

Table 4
Mean elastic modulus (standard deviation in parentheses).

Concrete type	E_c (GPa)
A0	44.3 (2.7)
A1	45.2 (0.6)
A2	44.9 (0.9)
A3	46.1 (1.0)

2.2.1. Slump flow, compressive strength and elastic modulus

To verify the self-compactness condition, slump flow tests were performed on fresh concrete [30]. One slump flow test per batch was carried out; that is, 4 per type of concrete. Table 2 shows the average results of the final diameter of the concrete poured (d_f), as well as the time to reach a diameter of 500 mm (t_{50}). A clear decrease in flowability is observed with increasing fiber content. This was to be expected since the only difference between the concrete types is the fiber dosage. Nevertheless, all concretes meet the self-compactness condition set in the Spanish Structural Code [31] (550 mm $\leq d_f \leq$ 850 mm). Moreover, a uniform distribution of fibers and coarse aggregate was observed in all cases, without segregation phenomena, exudation or other pathologies.

In hardened concrete the compressive strength was determined [32]. This parameter was obtained just before the beginning of the fatigue campaign, when the concrete reached an age of 1 year and 4 months. Four cylinders were tested for each type of concrete. Table 3 shows the average f_c results.

It can be noticed that the compressive strength is hardly affected by the fiber content. Other authors have obtained similar conclusions, pointing out that the addition of fibers, as well as an increase in their content, do not necessarily improve the compressive strength of concrete [33,34]. This is attributed to the balance between two opposing effects. On the one hand, the positive effect of the bridging forces generated by the fibers, reducing the occurrence and development of cracking. On the other hand, the negative effect of the reduction of flowability they induce, increasing porosity and pore size.

The overall mean value is 106.8 ± 2.1 MPa. Additionally, a batch of type A0 concrete was made to determine f_c at 28 days, obtaining an average value of 79.4 ± 1.8 MPa.

Finally, the modulus of elasticity in compression was determined [35]. Again, these tests were carried out before starting the fatigue tests. Three tests were performed for each type of concrete. Table 4 shows the mean values of E_c. It is observed that the variation of the modulus of elasticity with fiber content is statistically negligible. The overall mean value is 45.1 ± 1.5 GPa.

2.2.2. Static flexural strength

Static flexural tests to failure were also performed [7]. The difference between these tests and the previous ones is that these were used to characterize not only each concrete mix, but also each specimen size; in short, the 8 series mentioned above. The purpose of these tests is to determine the ultimate flexural strength, which in turn allows defining the load range of the fatigue tests.

The tests were carried out just before starting the fatigue campaign.

Fig. 3. Flexural test on specimens of size S (left) and L (right).

Table 5
Mean values of ultimate flexural strength, limit of proportionality and residual flexural strengths (in MPa). Fatigue stress levels (in MPa).

Series	σ_{ult}	f_L	f_{R1}	f_{R2}	f_{R3}	f_{R4}	$\sigma_{max,fat}$	$\sigma_{min,fat}$
A0-S	8.21	8.21	-	-	-	-	6.57	1.31
A0-L	5.23	5.23	-	-	-	-	4.18	0.84
A1-S	8.78	7.36	8.47	6.95	6.22	5.71	7.02	1.40
A1-L	5.93	5.22	5.12	5.11	5.02	4.50	4.74	0.95
A2-S	11.78	8.35	10.96	11.56	11.36	11.38	9.42	1.88
A2-L	11.37	6.67	9.95	10.81	10.79	9.79	9.10	1.82
A3-S	19.65	10.45	18.82	16.57	15.27	13.96	15.72	3.14
A3-L	16.41	7.74	15.19	16.14	15.32	14.34	13.13	2.63

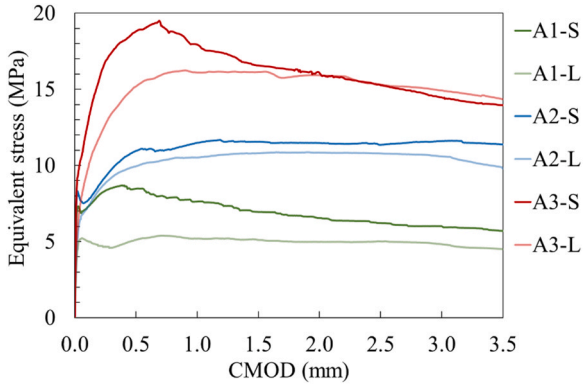

Fig. 4. Mean stress vs CMOD diagrams in series of SFRC.

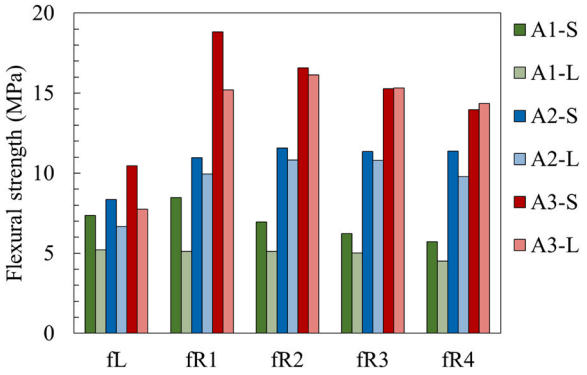

Fig. 5. Mean limit of proportionality and residual flexural strengths in series of SFRC.

Three prisms per series were tested. Since EN 14651 standard is designed for prisms of 150×150×600 mm (size L), for small specimens (size S) the test configuration was calculated following a proportional relationship: ratio between notch depth and specimen depth of 1/6, ratio between depth and length between supports of 0.3. Fig. 3 shows images of a bending test in each specimen size.

The parameters measured were the load, the relative displacement between the end supports and the central section, and the crack opening or CMOD. The load was recorded with a ± 50 kN load cell, model 661.20 F-02 (MTS, Eden Prairie, MN, USA). For the displacement, two high-precision laser distance meters with a range of 50 mm and an accuracy of 8 μm, model CP08MHT80 (Wenglor, Tettnang, Germany), were used. Finally, the CMOD was measured with an axial extensometer with a range of 25 mm and an accuracy of 10 μm, model 634.12 F-24, from MTS. The tests were carried out with displacement control, applying the load with a dynamic hydraulic actuator, model 244.21, from MTS. It is a double-acting cylinder with a range of ± 50 kN and a displacement amplitude of 150 mm.

Table 5 contains the mean values of the most relevant results: ultimate stress σ_{ult}, stress corresponding to the limit of proportionality f_L (according to EN 14651 [7]) and residual stresses f_{R1}, f_{R2}, f_{R3} and f_{R4} (according to MC 2010 [36], corresponding to CMOD values of 0.5, 1.5, 2.5 and 3.5 mm, respectively).

Due to the absence of fibers, in the plain concrete series (A0-S and A0-L), failure occurs when the first crack appears, for low CMOD values (≤ 0.05 mm). Therefore, σ_{ult} is equal to f_L and the concrete has no residual strength capacity.

It is observed that the ultimate flexural stress σ_{ult} clearly increases with fiber content. This is explained by the fact that the SFRC series, even from the lowest fiber content, show strain-hardening behavior. That is, the strength mechanism of the bridging forces of the fibers (post-cracking) has more capacity than that of the concrete matrix (pre-cracking). Therefore, it is verified that $\sigma_{ult} > f_L$.

This fact is more clearly seen in Fig. 4, where the mean stress vs CMOD diagrams in SFRC series are shown. In all cases σ_{ult} is reached at high CMODs (> 0.1 mm), when concrete has cracked and fibers have started to bear load. The only exception is A0-L series, where pre- and post-cracking mechanisms have practically the same strength.

Consequently, the higher the fiber content, the higher the bridging forces generated by the fibers and hence the strength of the concrete

Table 6
Cycles to failure in fatigue tests. Results with an asterisk indicate that the runout was reached.

Test No.	0% fibers		0.3% fibers		0.6% fibers		1.0% fibers	
	A0-S	A0-L	A1-S	A1-L	A2-S	A2-L	A3-S	A3-L
1	1000,000 *	767	6121	2626	3522	25,926	18,889	15
2	99,976	90	4838	899	10,316	37	918	23,308
3	511,248	143	3696	1830	40,858	3476	30	13
4	243,232	200	43	109	19,401	2004	3176	3335
5	139,687	263	2642	21,892	22,481	6597	12,888	15
6	456,365	594	2791	1255	1000,000 *	32	7195	5747
7	82,695	129	9226	134	26,308	8851	15,225	9604
8	2674	137	3956	284	20,746	46	12	3498
9	16,155	373	1512	69	5156	84	31	5634
10	1304	200	5263	102	5068	2415	3090	102
11	44,497	117	4015	18,876	14,233	4264	3743	1618
12	6153	258	48	42,491	5024	-	2219	12,964

after cracking increases.

Another interesting aspect is that all series show very good residual behavior; that is, they are able to maintain high stress levels even for large CMODs, up to 3.5 mm or even higher. This is seen in Fig. 5, where the average residual stresses are plotted. If the ratio f_{R3}/f_{R1}, used in MC 2010 to characterize the residual behavior of SFRC, is calculated, it is obtained that in all series, except for A1-S and A3-S, its value is higher than 1. This proves the high residual capacity of the material.

2.3. Fatigue tests

Once the concrete was characterized, cyclic three-point bending tests were carried out until failure. The prisms used in these tests are geometrically identical to those used in the static tests. 12 tests were conducted per series, i.e., per specimen size and type of concrete. In total, the fatigue campaign comprised 96 tests.

In each series, cycles with constant stress levels were applied until specimen failure occurred. To define the stress levels, the average value of the ultimate flexural strength (σ_{ult}) in each series was taken as a reference. In all cases, cyclic loads between 16% and 80% of σ_{ult} were applied, i.e., with a stress ratio of 0.2. Therefore, all series were subjected to the same relative stress levels, thus negating the influence of fiber content on the static flexural response. Table 5 shows the stress levels $\sigma_{max,fat}$ and $\sigma_{min,fat}$ (or simply σ_{max} and σ_{min}) of all series. It can be seen that, the higher the fiber content, the higher the σ_{ult} and therefore the higher the stress levels in absolute value. However, the ratios $\sigma_{max}/\sigma_{ult}$ and $\sigma_{min}/\sigma_{ult}$ remain constant.

The frequency of the load cycles was 5 Hz. In addition, a runout limit of 10^6 cycles was established. This value responds to two reasons. On the one hand, the relative stress levels (16%−80% of σ_{ult}) were set assuming a target fatigue life of 10^4 cycles, for which an extensive literature consultation of similar experimental campaigns was made [37–42]. On the other hand, a dispersion of results of up to two orders of magnitude, usual in concrete fatigue, was considered.

Regarding the parameters measured and the sensorics placed, everything described about static bending tests in subsection 2.2.2 is applicable. The only additional parameter recorded was obviously the number of cycles to failure.

3. Results and discussion

3.1. Size effect in static flexural strength

Fig. 4 shows that there is a noticeable size effect on the static flexural response. That is, S specimens show higher flexural strength than L specimens. This size effect occurs not only in SFRC series, but also in PC. Table 5 reveals that there is an increase in strength both in terms of ultimate flexural stress σ_{ult} and limit of proportionality stress f_L. Consequently, there is a size effect associated with the pre-cracking mechanism, governed by the matrix, and another one related to the post-cracking mechanism, dominated by the fibers.

Considering the ultimate flexural stress σ_{ult}, the most pronounced size effect occurs in PC series (A0-S and A0-L), where its value is 57% higher in small specimens. In SFRC series, these percentages are 48%, 4% and 20% for series with 0.3%, 0.6% and 1% fibers, respectively. Therefore, the smallest size effect occurs in the A2-S and A2-L series, as can be seen in Fig. 4.

The size effect observed in PC series, as well as in the f_L in SFRC series, where fibers hardly intervene, can be explained from the point of view of fracture mechanics, through the size effect law (SEL) of Bažant [3] (Fig. 1). When a concrete element cracks, a microcracking area called fracture process zone (FPZ) is generated at the crack front. The length of the FPZ is a material constant, so that small elements have a ductile fracture behavior, while large elements are more brittle. It appears that the two sizes considered in this work are in the ductile-brittle transition region of the SEL, which causes the smaller specimens to have higher flexural strength.

With respect to the size effect in SFRC series, particularly in cracked situation, it is not expected that the size effect of fracture mechanics would be so significant. This is because in SFRC the length of the FPZ is much longer, due to the ductility provided by the bridging forces of the fibers. This means that in Fig. 1 the SEL curve would be shifted to the right. Thus, it is possible that in PC the two specimen sizes studied are located in the ductile-fragile transition, while in SFRC they are placed in the ductile section, with a much less pronounced size effect.

The predominant cause that can explain the size effect in SFRC is the fiber wall effect. In small specimens the fibers tend to align longitudinally in a more pronounced way than in large specimens. This can be quantified by the ratio of fiber length to minimum element dimension, which is 0.4 for S specimens and 0.2 for L specimens. The higher the value, the greater the wall effect and thus the greater the influence of specimen geometry on fiber distribution. Consequently, in S specimens the fibers are better oriented to withstand bending stresses, causing an increase in σ_{ult}.

3.2. Size effect in flexural fatigue behavior

3.2.1. Fatigue life

Table 6 shows the fatigue life N of the 12 specimens of each series. It is worth mentioning that in A2-L series one specimen was lost due to an incidence in the test control.

It is observed that there is a strong size effect in PC series (A0-S and A0-L). The larger specimens have a significantly lower fatigue life than the smaller ones, the difference being several orders of magnitude. While in no case in A0-L series 10^3 cycles are exceeded, in A0-S series 10^5 cycles are exceeded up to 5 times; in fact, one of the specimens reached the runout of 10^6 cycles.

With respect to SFRC series, it appears that the size effect is much less

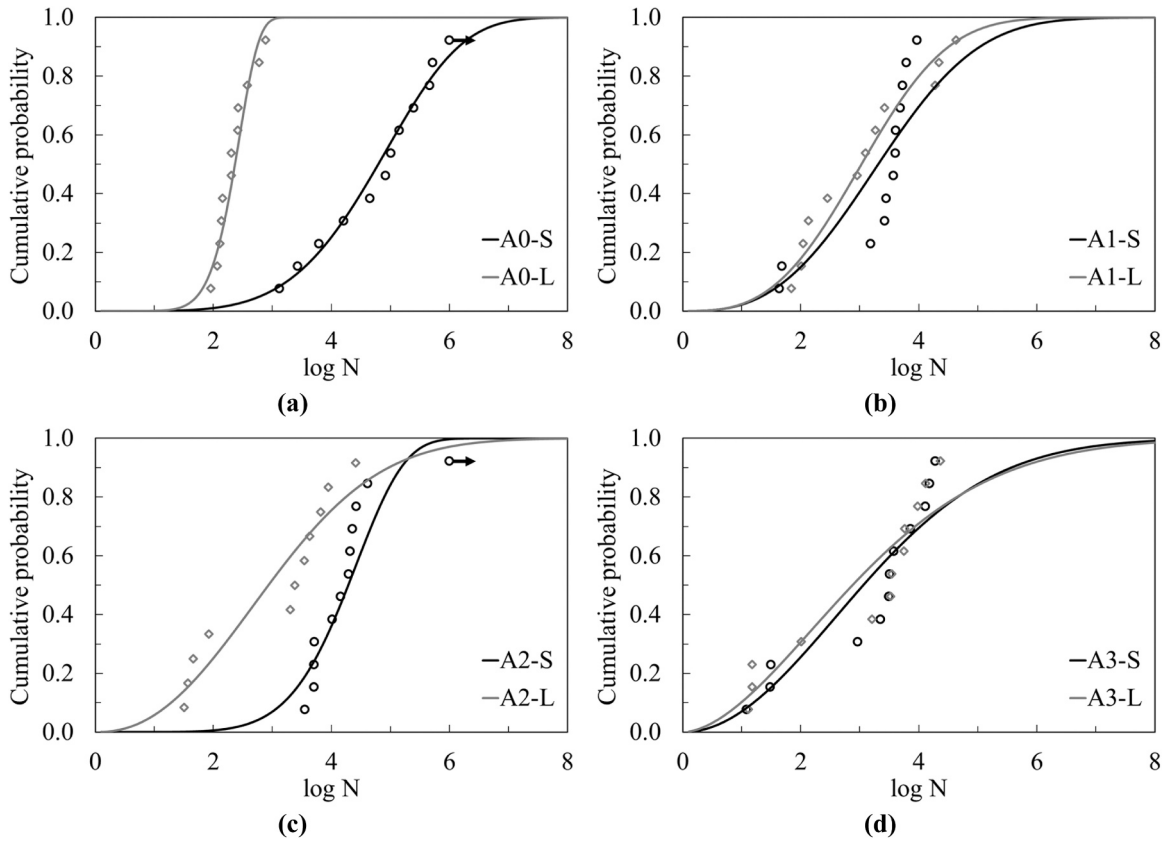

Fig. 6. Fitting of Weibull distribution function to fatigue life results in series with 0% (a), 0.3% (b), 0.6% (c) and 1% (d) fibers.

Table 7
Parameters of the Weibull function fit to N.

Fibers (%)	Series	λ	β
0%	A0-S	5.17	4.80
	A0-L	2.47	8.16
0.3%	A1-S	3.76	2.87
	A1-L	3.42	3.02
0.6%	A2-S	4.54	6.35
	A2-L	3.44	2.28
1.0%	A3-S	3.67	2.01
	A3-L	3.54	1.76

pronounced. In fact, only in A2-S and A2-L series, with 0.6% fibers, it is noticed that the fatigue life is clearly higher in small specimens than in the large ones. It should be noted that, although the survival limit was reached in one test of A2-S series, this result could be considered anomalous, since the next specimen that withstood the most cycles has an N two orders of magnitude lower.

Due to the large scatter in fatigue results, it is common to use probability models to statistically describe the data. In particular, the two-parameter Weibull distribution function is the most widely used, fitting reasonably well to both compressive and flexural fatigue data, and both PC and SFRC [39,43]. The cumulative Weibull distribution function can be expressed as:

$$F(x) = 1 - \exp\left\{ -(x/\lambda)^{\beta} \right\} \quad (1)$$

where x is log(N), β is the shape parameter and λ is the scale parameter. The first is related to the dispersion, such that, the larger β is, the smaller the variability of the data. The second is related to the characteristic fatigue life, so that, the larger λ, the larger the fatigue life.

Fig. 6 shows the Weibull fits to the N results for all series, separated by fiber content. Table 7 contains the values of the fit parameters.

Fig. 6.a reveals an obvious size effect in PC series since the fit curve of A0-S series is much more to the right of that of A0-L series. The difference is close to three orders of magnitude, as denoted by the values of the scaling parameter λ, indicative of the characteristic fatigue life (Table 7). As for the dispersion of results, it is noteworthy that in A0-L series it is particularly low; in fact, it is the series with the lowest dispersion (highest β), with almost all its data being grouped in one order of magnitude (between 10^2 and 10^3). In contrast, A0-S series presents a higher variability, although within the usual range for concrete fatigue.

With respect to the series with the lowest fiber content, Fig. 6.b shows that the fatigue life of A1-S series is only slightly higher than that of A1-L series, as seen in the similar λ values (Table 7). In addition, the dispersion is a little higher in A1-S series, with a flatter curve and consequently a lower β. In this regard, it is worth mentioning that in this series the two tests with a lower N (43 and 48 cycles) alter the fit very noticeably, since the rest of the values are between 10^3 and 10^4 cycles.

The series with a fiber dosage of 0.6% show the most pronounced size effect among all SFRC series, as shown in Fig. 6.c. However, its magnitude is far from that observed in PC series. It is seen that A2-S series has a characteristic fatigue life of about one order of magnitude higher than that of A2-L series (Table 7). On the other hand, the dispersion of the results is relatively low in A2-S series, hardly altered by the anomalous test that exceeded the runout limit. Meanwhile, A2-L series presents a higher variability, and it is observed that the fit is disturbed by a group of tests with particularly low fatigue lives ($< 10^2$ cycles).

Finally, Fig. 6.d shows that the series with the largest quantity of fibers have practically identical fatigue lives, with a λ of 3.67 and 3.54 for A3-S and A3-L, respectively (Table 7). Therefore, it can really be stated that no size effect is observed in this case. With respect to dispersion, again it is very similar, being slightly lower in A3-S series.

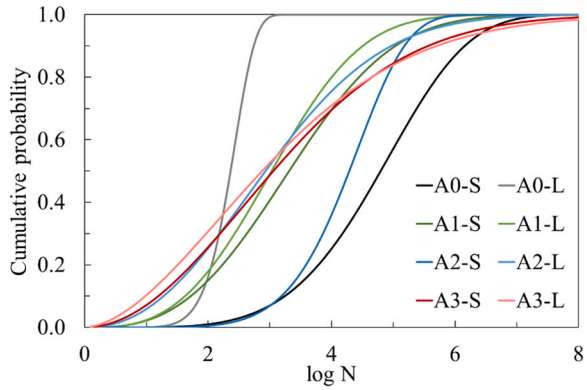

Fig. 7. Fitting of Weibull distribution function to fatigue life results in all series.

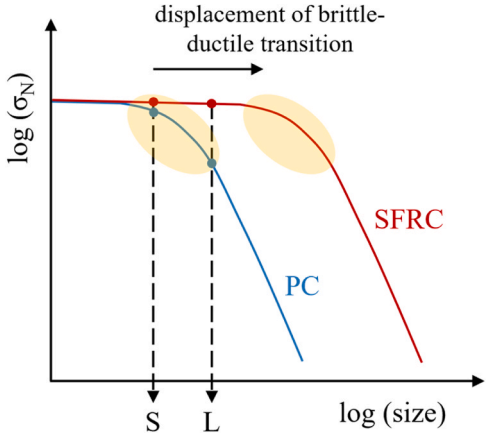

Fig. 8. Strength-size curves in plain concrete and fiber-reinforced concrete, and their influence on the size effect.

Once again, the fits are altered by the lower fatigue life results, although it affects both series equally.

Next, in Fig. 7 the Weibull fits of all series are plotted simultaneously. For ease of interpretation, the dots indicating each individual test have been omitted.

Fig. 7 yields interesting conclusions. First, the addition of fibers reduces the size effect. In fact, it could be said that it practically eliminates it, since the difference in N between the two specimen sizes goes from 3 orders of magnitude in PC to almost zero in SFRC with fiber contents of 0.3% (A1-S and A1-L series) and 1% (A3-S and A3-L series). Only in the series with 0.6% of fibers is there a notable size effect, with the small specimens having a characteristic fatigue life of about one order of magnitude greater than that of the large ones.

In relation to the above, the decrease in the size effect is not proportional to the fiber content. It seems that 0.3% of fibers is sufficient to nullify the size effect, and that thereafter an increase in the dosage does not cause substantial improvements. As for the size effect of the 0.6% fiber series, it can be explained because the results of A2-S series are statistically different from the rest; in particular, no result is less than 10^3 cycles, which reduces the dispersion (see high value of β in Table 7) and thus raises the characteristic fatigue life. If the number of tests were higher, it is likely that low fatigue life results would appear and consequently the curve of A2-S series would be much more similar to that of the rest of SFRC series.

The explanation of why the size effect on fatigue life occurs in PC and not in SFRC lies again in the fracture mechanics of concrete. It is likely that, in the case of PC, the two specimen sizes tested are in the brittle-ductile behavior transition zone (Fig. 8). In this region of the strength-size curve, a clear size effect takes place, which causes both the static flexural strength and fatigue life to be higher in the small specimens than in the large ones. On the other hand, by adding fibers, the deformation capacity of the material is greatly increased (even for low fiber contents). In short, SFRC is much more ductile than PC. The practical result is that the strength-size curve of SFRC is shifted to the right (Fig. 8). Consequently, the same specimen sizes that in PC were affected by the size effect, in SFRC are in the plastic region (upper horizontal asymptote), not influenced by the size effect. This is the reason why in all SFRC series the fatigue life is similar and independent of size. Regarding the size effect on the static flexural strength of SFRC, it should be remembered that in this case the wall effect of the fibers plays a role, which causes the fibers to be better aligned in the S specimens and therefore their strength increases. However, in fatigue tests, as each series is subjected to the same relative stress levels, the differences in static strength between sizes, and therefore this wall effect, are eliminated.

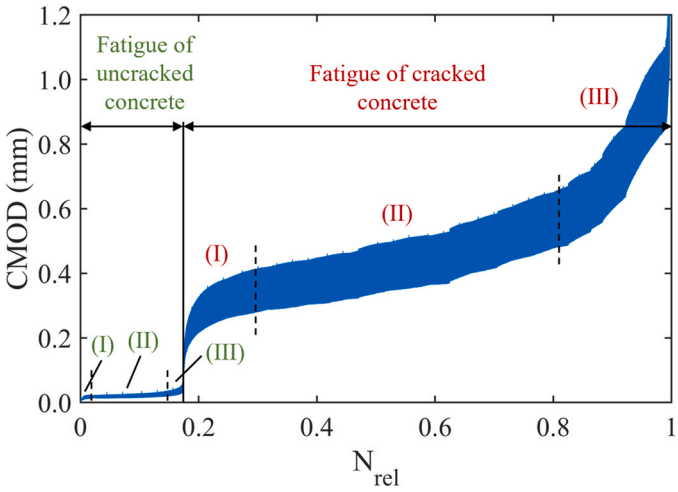

Fig. 9. CMOD vs relative N plot in an A1-S series test (SFRC with 0.3% fibers). Differentiation of the two fatigue mechanisms observed.

Finally, other relevant conclusions can be drawn from Fig. 7 that are not directly related to the size effect. It is observed that the addition of fibers does not necessarily improve the fatigue strength. In fact, the trend changes depending on the specimen size. While in S specimens PC series has the highest fatigue life and its value decreases in all SFRC series, the opposite situation occurs in L specimens. Another interesting aspect is that the fiber content hardly influences the flexural fatigue life, at least for the dosages used. With the exception of A2-S series, where the results differ from the rest, the fit curves of SFRC series are practically coincident, with no clear trends observed in any of the two specimen sizes.

3.2.2. *Cyclic creep curves*

In addition to the fatigue life, it is interesting to study the evolution of damage due to cyclic loading. For this purpose, cyclic creep curves are resorted to, which represent the crack opening at the maximum stress level σ_{max} versus the number of cycles [39,44]; in other words, the upper envelope of the CMOD vs N diagram.

In both PC and SFRC, these curves have a characteristic S-shape, dividing into three stages. However, the damage mechanism involved in each material is quite different. On the one hand, in PC, fatigue of uncracked concrete occurs, governed by the matrix and characterized by the following stages: (I) plastic tensile deformation and birth of scattered microcracking around the notch edge, (II) stable growth of microcracks, and (III) convergence into a main macrocrack that triggers failure. On the other hand, fatigue of cracked concrete develops in SFRC, dominated by fibers and consisting of these stages: (I) concrete cracking and fiber loading, (II) stable progression of the main macrocrack by progressive

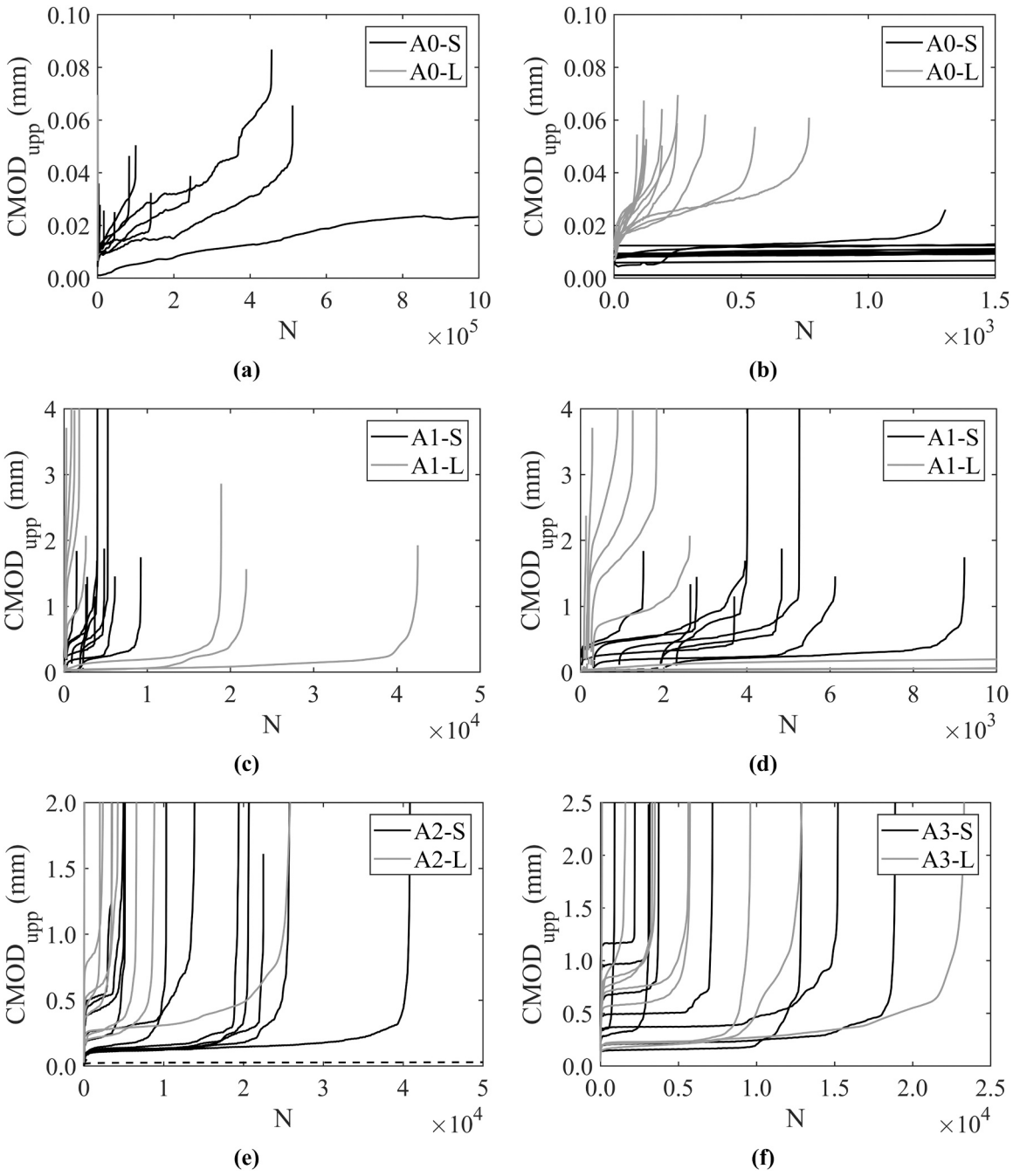

Fig. 10. Cyclic creep curves in PC series (a-b) and SFRC series with fiber contents of 0.3% (c-d), 0.6% (e) and 1% (f). Note:.

fiber failure, and (III) unstable propagation of the macrocrack until failure.

It should be pointed out that, while in PC only fatigue of uncracked concrete occurs, in SFRC both mechanisms may be involved. Specifically, this is usually observed when the maximum stress level σ_{max} is lower than the first crack stress (similar to the stress of the limit of proportionality f_L). In these cases, the cyclic creep curve is formed by a double S-curve: the first one associated with the fatigue of uncracked concrete, and the second one, with fatigue of cracked concrete [45]. Fig. 9 shows the CMOD vs relative number of cycles plot in an A1-S series test where this double behavior is observed. The two fatigue mechanisms are differentiated, as well as the stages that constitute them.

Fig. 10 shows the cyclic creep curves of all fatigue tests, divided by concrete type. In each graph, the curves of the S-size specimens are shown in black, while those of the L-size specimens are plotted in gray. Tests with a very small fatigue life (< 50 cycles) have not been plotted. It should be noted that, in those SFRC tests where the two aforementioned fatigue mechanisms have been observed, the section associated with the fatigue of uncracked concrete has been represented in dashed line. This is mainly seen in the series with the lowest fiber content (A1-S and A1-L). Fig. 10.b and d represent the same data as in Fig. 10a and c, respectively, but with the X-axis range adjusted to properly observe the curves of specimens with lower fatigue lives.

Fig. 10.a and b show that the fatigue life of A0-S series is much larger than that of A0-L series, as discussed in the previous subsection. The cyclic creep curves can help to understand this strong size effect. It can be seen that, in both series, stage (II) is the longest and the one that governs the evolution of fatigue damage. This section is approximately linear, so it can be characterized through a single parameter: the slope of its line of best fit. As a preliminary conclusion, it is noted that the slope

Table 8
Fatigue life in series with 0.3% of fibers, divided by type of fatigue mechanism.

Test No.	A1-S			A1-L		
	N_{mat}	N_{fib}	N	N_{mat}	N_{fib}	N
1	346	5775	**6121**	301	2325	**2626**
2	1924	2914	**4838**	196	703	**899**
3	31	3665	**3696**	260	1570	**1830**
4	27	16	**43**	92	17	**109**
5	1948	694	**2642**	-	21,892	**21,892**
6	49	2742	**2791**	138	1117	**1255**
7	2118	7108	**9226**	82	52	**134**
8	327	3629	**3956**	158	126	**284**
9	17	1495	**1512**	65	4	**69**
10	934	4329	**5263**	89	13	**102**
11	2305	1710	**4015**	-	18,876	**18,876**
12	42	6	**48**	-	42,491	**42,491**

Table 9
Fatigue life in series with 0.6% of fibers, divided by type of fatigue mechanism.

Test No.	A2-S			A2-L		
	N_{mat}	N_{fib}	N	N_{mat}	N_{fib}	N
1	59	3463	**3522**	-	25,926	**25,926**
2	504	9812	**10,316**	-	37	**37**
3	50	40,808	**40,858**	-	3476	**3476**
4	57	19,344	**19,401**	-	2004	**2004**
5	53	22,428	**22,481**	-	6597	**6597**
6	1000,000	-	**1000,000**	-	32	**32**
7	56	26,252	**26,308**	-	8851	**8851**
8	-	20,746	**20,746**	-	46	**46**
9	-	5156	**5156**	-	84	**84**
10	-	5068	**5068**	-	2415	**2415**
11	-	14,233	**14,233**	-	4264	**4264**
12	-	5024	**5024**			

of stage (II) is clearly greater in large specimens, i.e., fatigue damage is faster. Consequently, this fact, added to the one that the ultimate CMOD is similar in both sizes, could explain the shorter fatigue life in L specimens.

It is worth mentioning that the slope of stage (II) is known as the secondary crack opening rate (dCMOD/dn) [40], and will be discussed in detail in the next subsection.

Secondly, Fig. 10.c and d reveal that in the series with 0.3% fibers, the two explained fatigue mechanisms appear: fatigue of uncracked concrete (or of the matrix) and fatigue of cracked concrete (or of the fibers). Consequently, the fatigue life can be divided into two sections, named N_{mat} and N_{fib}, respectively (Table 8).

From Table 8 it can be concluded that the fatigue life is slightly higher in the small specimens. In A1-S series, N exceeds 10^3 cycles on 10 occasions, while in A1-L series it does so only on 6 occasions. However, it is noteworthy that the three tests with more N belong to A1-L series, exceeding 10^4 cycles. Precisely these specimens are the only ones in this series in which only fatigue of cracked concrete has intervened; that is, the only ones that have cracked after the first loading cycle.

Again, the dispersion of fatigue life in general, and the size effect in particular, can be explained through the cyclic creep curves. There seems to be a relationship between the slope of stage (II) in fatigue of cracked concrete, denoted $(dCMOD/dn)_{fib}$, and fatigue life. The higher the $(dCMOD/dn)_{fib}$, the lower the N (Fig. 10.d). In this case, fatigue of uncracked concrete has little impact because, with few exceptions, N_{mat} is small compared to N_{fib} (Table 8).

In addition, there is another part of the curves that seems to affect fatigue life: the transition zone between the fatigue of uncracked and cracked concrete. It is clearly seen that in A1-L series specimens, the increase in CMOD that occurs from the time the concrete cracks until the fibers are mobilized is very high, about 1 mm or even higher (Fig. 10.d). In contrast, in A1-S series the CMOD jump is much smaller, practically

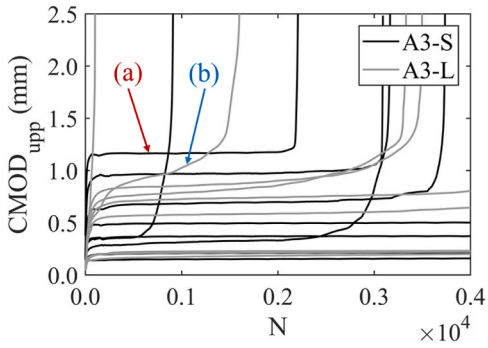

Fig. 11. Cyclic creep curves in SFRC series with fiber contents of 1% (detail view).

not exceeding 0.5 mm. It is observed that the higher the CMOD increase in the transition zone, the lower the fatigue life. In fact, this would explain the higher N of the three A1-L series specimens, which do not have a transition zone.

In the third place, in the tests with 0.6% fibers, both fatigue mechanisms are also observed. However, as shown in Table 9, the sections of fatigue of uncracked concrete only appear in some specimens of A2-S series and are very small in relation to the total fatigue life. This is explained because in both series it is satisfied that $\sigma_{max} > f_L$, so it is to be expected that the concrete will crack from the first cycle. The only exception is a test of A2-S series that has reached the survival limit of 10^6 cycles, which as explained is considered anomalous.

Fig. 10.e and Table 9 reveal a clear size effect. It can be seen that no test in A2-S series is below 10^3 cycles, something that is only repeated in A0-S series, the one with the best fatigue behavior of all. At the same time, in A2-L series there are up to four specimens with a very low N, below 10^2 cycles.

Some interesting conclusions can be drawn from Fig. 10.e. As already seen in the other series, a relationship between $(dCMOD/dn)_{fib}$ and N is observed; that is, the higher the slope of stage (II) of the cyclic creep curves, the lower the fatigue strength. Moreover, it is also observed that, when the initial CMOD of stage (II) (denoted as $CMOD_{II,i}$) is larger, the fatigue life is reduced. In fact, it is noticed that the tests of both series with less N are those with the highest $CMOD_{II,i}$, above 0.3–0.4 mm. In general, the value of this parameter is markedly higher in A2-L series. Consequently, the combination of high $(dCMOD/dn)_{fib}$ and $CMOD_{II,i}$ could explain the size effect in the series with 0.6% fibers.

A relationship between the two parameters is observed, so that the higher the $CMOD_{II,i}$, the higher the dCMOD/dn; that is, if the crack stabilizes with a higher CMOD and the effective resistant section is reduced, the speed of fatigue damage increases, which has a certain logic. However, this is not exactly fulfilled, since specimens with a low $CMOD_{II,i}$ have higher dCMOD/dn than others with a higher $CMOD_{II,i}$, both within the same series and comparing between the two sizes.

Finally, in the series with 1% fibers only the fatigue mechanism of cracked concrete is involved; that is, since σ_{max} is much larger than f_L, in all cases concrete cracks after the first cycle.

Fig. 10.f shows that the fatigue life in the two specimen sizes is very similar, as discussed in the previous subsection.

Although there is no size effect in this case, cyclic creep curves can be used to explain the dispersion of the results, i.e., why some specimens withstand more cycles than others. As in the series with 0.6% fibers, there seems to be a relationship between fatigue life and two parameters: the secondary crack opening rate dCMOD/dn and the crack opening at the beginning of stage (II) $CMOD_{II,i}$. The higher their values, the lower N. In some cases, as in test (a) in Fig. 11, the low fatigue life is explained by a high $CMOD_{II,i}$, while dCMOD/dn is lower even than in other specimens of the same series that have lasted more cycles. In other cases, as in test (b) in Fig. 11, the reduced N is due to a high dCMOD/dn, even

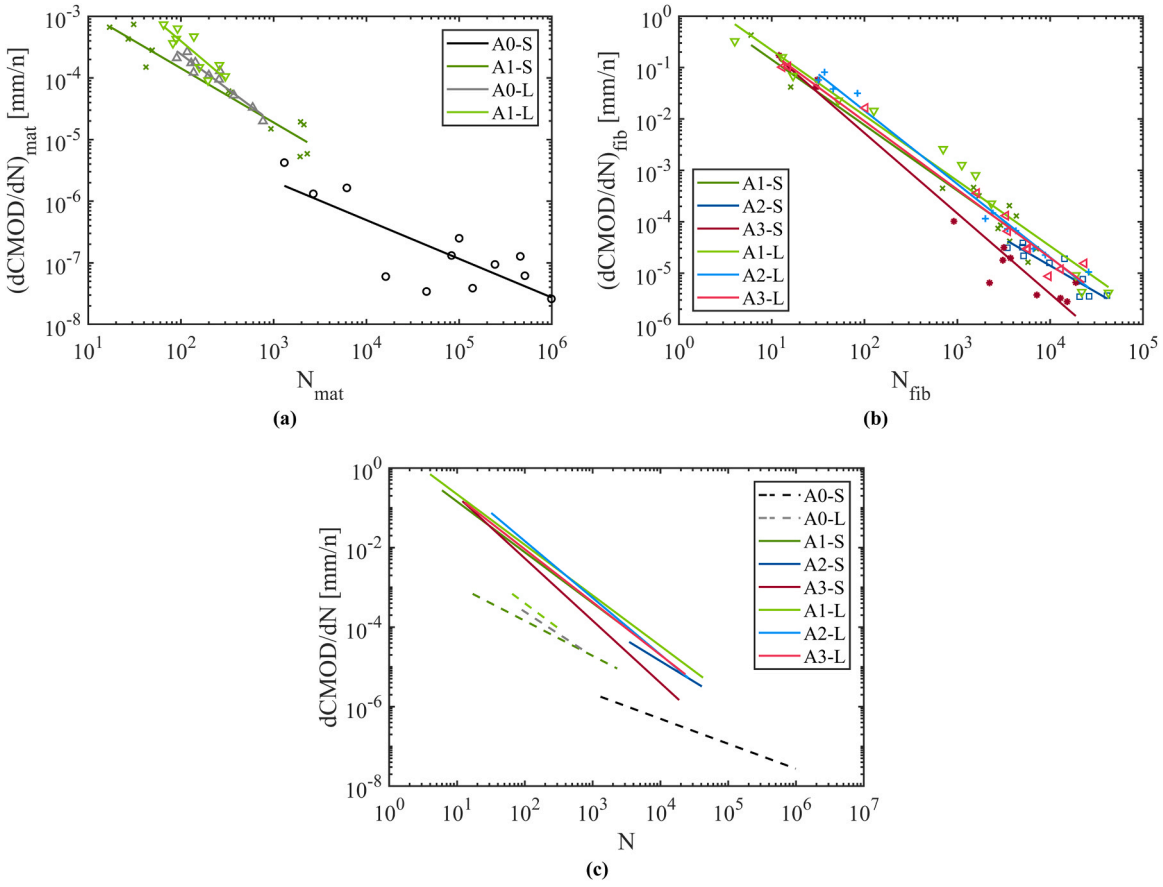

Fig. 12. Secondary crack opening rate (dCMOD/dn) vs fatigue life: (a) PC series and SFRC series sections with uncracked concrete fatigue, (b) SFRC series sections with cracked concrete fatigue, (c) sections of both fatigue mechanisms together.

Table 10
Secondary crack opening rates in sections of uncracked concrete fatigue, $(dCMOD/dn)_{mat}$.

Test No.	0% fibers		0.3% fibers	
	A0-S	A0-L	A1-S	A1-L
1	2.60E-08	1.99E-05	5.83E-05	1.06E-04
2	2.50E-07	2.11E-04	5.29E-06	9.10E-05
3	6.18E-08	1.79E-04	7.41E-04	1.61E-04
4	9.42E-08	1.10E-04	4.27E-04	6.35E-04
5	3.88E-08	1.30E-04	1.94E-05	-
6	1.27E-07	3.31E-05	2.82E-04	4.71E-04
7	1.31E-07	1.75E-04	1.74E-05	3.66E-04
8	1.32E-06	1.22E-04	6.12E-05	1.49E-04
9	5.98E-08	5.23E-05	6.64E-04	7.37E-04
10	4.22E-06	1.11E-04	1.50E-05	4.29E-04
11	3.42E-08	2.65E-04	5.89E-06	-
12	1.64E-06	9.43E-05	1.50E-04	-

though they present comparatively moderate $CMOD_{II,i}$. Consequently, this could indicate that the two parameters have a certain degree of independence, being their combination what determines the fatigue response of each specimen.

3.2.3. Secondary crack opening rate

Cyclic creep curves are usually characterized through a single parameter: the slope of stage (II), which is approximately linear and which, being the most extensive, controls the evolution of fatigue damage. This is known as the secondary crack opening rate dCMOD/dn. Some authors point out that there is a good correlation between the logarithms of dCMOD/dn and fatigue life [39,40], although few works address this in depth. This relationship was initially proposed by Sparks & Menzies [46] in compressive fatigue, where it is well known and it is demonstrated that, the higher the secondary strain rate (dε/dn), the

Table 11
Secondary crack opening rates in sections of cracked concrete fatigue, $(dCMOD/dn)_{fib}$.

Test No.	0.3% fiber		0.6% fibers		1.0% fibers	
	A1-S	A1-L	A2-S	A2-L	A3-S	A3-L
1	1.63E-05	2.26E-04	3.11E-05	1.05E-05	6.55E-06	1.04E-01
2	8.58E-05	2.59E-03	1.58E-05	8.11E-02	1.02E-04	1.55E-05
3	4.18E-05	8.03E-04	3.65E-06	7.28E-05	4.17E-02	1.02E-01
4	4.19E-02	6.88E-02	6.95E-06	1.15E-04	3.14E-05	1.31E-04
5	4.46E-04	4.30E-06	7.62E-06	2.98E-05	3.26E-06	1.05E-01
6	7.43E-05	1.27E-03	-	5.73E-02	3.74E-06	2.92E-05
7	3.00E-05	2.28E-02	3.55E-06	2.25E-05	2.78E-06	8.69E-06
8	2.06E-04	1.44E-02	3.48E-06	3.82E-02	1.72E-01	6.54E-05
9	4.64E-04	3.26E-01	2.16E-05	3.16E-02	5.78E-02	2.99E-05
10	1.30E-04	1.59E-01	3.87E-05	1.48E-04	1.78E-05	1.64E-02
11	3.20E-04	9.08E-06	1.90E-05	6.66E-05	1.97E-05	3.61E-04
12	4.28E-01	4.14E-06	3.18E-05		6.49E-06	1.19E-05

lower the number of cycles to failure.

Fig. 12 shows the linear regressions between the logarithms of dCMOD/dn and N. In those series where a double fatigue mechanism appears (A1-S and A1-L), two crack opening rates can be identified; namely, $(dCMOD/dn)_{mat}$ and $(dCMOD/dn)_{fib}$. The former corresponds to the first fatigue mechanism, where the concrete has not yet cracked, while the latter corresponds to the second fatigue mechanism, where the concrete has already cracked. Each crack opening rate ($(dCMOD/dn)_{mat}$ and $(dCMOD/dn)_{fib}$) has been correlated with its corresponding number of cycles (N_{mat} and N_{fib}). This is the reason why A1-S and A1-L series appear in the plots of fatigue of uncracked concrete (Fig. 12.a) and cracked concrete (Fig. 12.b). In this regard, the sections of fatigue of uncracked concrete in A2-S series have been discarded since they are unrepresentative.

In addition, Tables 10 and 11 contain the values of the secondary crack opening rates, separated by type of fatigue mechanism.

Fig. 12.a reveals that there is a good correlation between dCMOD/dn and N in both PC series and the sections of fatigue of uncracked concrete in SFRC series. It is verified that, the higher the secondary crack opening rate, the lower the fatigue life. In addition, it is observed that in general terms, the regression lines of SFRC series follow a very similar trend to those of PC. This would indicate that the evolution of fatigue damage of uncracked concrete is essentially the same in the two classes of concrete, which would confirm the statement that fibers are hardly involved in this type of fatigue.

On the one hand, with respect to PC series, it is noticed that the strong size effect is explained by the fact that $(dCMOD/dn)_{mat}$ in much smaller in A0-S series. In other words, the damage inflicted by cyclic loading is slower in the small specimens, causing the fatigue life to be longer. On the other hand, in the series with 0.3% fibers, it can be seen that the straight lines are appreciably parallel, indicating that the relationship between $(dCMOD/dn)_{mat}$ and N_{mat} follows the same proportion; that is, a certain increase in $(dCMOD/dn)_{mat}$ produces the same decrease in N_{mat}. Although no clear size effect is observed in these series, the secondary crack opening rate would explain the dispersion of the results.

In the second place, Fig. 12.b shows that there is a very strong correlation between $(dCMOD/dn)_{fib}$ and N_{fib}, following the expected trend; that is, an increase in $(dCMOD/dn)_{fib}$ causes a decrease in fatigue life. It is noteworthy that all the regression lines are practically coincident. Therefore, this would indicate that the relationship between dCMOD/dn and N in fatigue of cracked concrete is independent, not only of fiber content, but also of specimen size. Evidently, this is demonstrated for the values used in this work, pending validation for wider ranges of fiber dosages and element dimensions.

In any case, it is shown that the secondary crack opening rate is a very adequate parameter to explain the dispersion of N in flexural fatigue of concrete.

With respect to the series with 0.6% fibers, which are the only SFRC series in which there is a significant size effect, it can be seen that all the tests of A2-S series present reduced $(dCMOD/dn)_{fib}$, less than 10^{-4} and concentrated in the lower right part of the graph. Therefore, this parameter again explains the size effect.

Finally, Fig. 12.c reveals that the lines corresponding to the fatigue of cracked concrete (in solid line) are above those of fatigue of uncracked concrete (in dashed line), i.e., the fatigue mechanism governed by fibers damages concrete faster than the one dominated by the matrix. This is to be expected, since the fibers provide much ductility, making the concrete admit large deformations, as seen in the $CMOD_{upp}$ vs N diagrams (Fig. 10.c to f). For the same fatigue life, the difference between $(dCMOD/dn)_{mat}$ and $(dCMOD/dn)_{fib}$ is about one order of magnitude. Since the two sets of straight lines are approximately parallel, this difference remains roughly constant over the entire range of N observed. This is the same conclusion reached by Germano et al. [40].

4. Conclusions

In this work, an experimental study of the size effect on flexural fatigue in concrete is carried out. For this purpose, prismatic specimens of two sizes have been manufactured: 75×75×300 mm (S) and 150×150×300 mm (L). As the main objective is to assess the size effect depending on the addition and content of fibers, four types of concrete have been produced: plain and steel fiber-reinforced with contents of 0.3%, 0.6% and 1% of fibers. Therefore, a total of eight series of specimens were tested. All specimens were subjected to 3-point bending fatigue at the same relative stress levels.

The main conclusions of the investigation are summarized below:

- A clear size effect is observed in the static flexural strength in all series, both PC and SFRC. It is shown that the stress at the limit of proportionality (f_L) and ultimate stress (σ_{ult}) are higher in specimens S. The size effect of f_L is attributed to the fracture mechanics of concrete, by means of Bažant's SEL. The σ_{ult} size effect in the SFRC series is explained by the wall effect, which causes the fibers to be better oriented in the S specimens.
- It is concluded that the addition of fibers mitigates the size effect of fatigue life. While in PC the S specimens have a fatigue life up to 3 orders of magnitude higher than that of the L specimens, in SFRC this difference practically disappears. This is because fibers increase the ductility of the material, moving away the brittle-ductile transition in SFRC, which makes it less sensitive to the size effect.
- Fibers do not necessarily improve the fatigue life of concrete. In fact, the trend changes depending on the specimen size: in S specimens the PC series withstands more cycles, while in L specimens the opposite is true.
- In the cyclic creep curves, it can be seen that the higher the slope of stage (II), called secondary crack opening rate dCMOD/dn, the lower the fatigue life. This is known as the Sparks & Menzies relationship and is fulfilled in both PC and SFRC. Consequently, the parameter dCMOD/dn is able to explain the fatigue life dispersion in general, and the size effect in particular.

CRediT authorship contribution statement

González Dorys C.: Writing – review & editing, Resources, Methodology, Investigation, Funding acquisition. **Mínguez Jesús:** Writing – review & editing, Resources, Methodology. **Vicente Miguel A.:** Writing – review & editing, Supervision, Resources, Funding acquisition, Conceptualization. **Mena-Alonso Alvaro:** Writing – review & editing, Writing – original draft, Methodology, Investigation, Formal analysis.

Declaration of Competing Interest

The authors declare that they have no known competing financial interests or personal relationships that could have appeared to influence the work reported in this paper.

Data availability

The data that has been used is confidential.

Acknowledgments

The authors are grateful for the financial support of the Spanish Ministerio de Economía y Competitividad (grant no. PID2019–110928RB-C32) and the Spanish Ministerio de Ciencia, Innovación y Universidades (grant no. FPU19/02685).

References

[1] EN 1992–1-1, Eurocode 2: Design of concrete structures - Part 1–1: General rules and rules for buildings, 1991.
[2] C. Ríos, J.C. Lancha, M.Á. Vicente, Fatigue in structural concrete according to the new eurocode 2, Hormig. Y. Acero (2023), https://doi.org/10.33586/hya.2023.3100.
[3] Z.P. Bažant, Size effect on structural strength: a review, Arch. Appl. Mech. 69 (1999) 703–725, https://doi.org/10.1007/s004190050252.
[4] Z.P. Bažant, J. Planas, Fracture and Size Effect in Concrete and Other Quasibrittle Materials, Taylor & Francis,, 1998, https://doi.org/10.1201/9780203756799.
[5] H. Cifuentes, F. Medina, Mecánica de la fractura aplicada al hormigón. Conceptos, análisis experimental y modelos numéricos, Secretariado de Publicaciones. Universidad de Sevilla, 2013.
[6] ASTM C1609/C1609M-12. Standard Test Method for Flexural Performance of Fiber-Reinforced Concrete (Using Beam With Third-Point Loading), 2012.
[7] UNE-EN 14651:2007+A1, Método de ensayo para hormigón con fibras metálicas, Determinación De. la Resist. a la Tracc. por flexión (límite De. proporcionalidad (LOP), Resist. residual (2008).
[8] V.C. Li, Z.L. Lin, T. Matsumoto, Influence of fiber bridging on structural size-effect, Int J. Solids Struct. 35 (1998) 4223–4238, https://doi.org/10.1016/S0020-7683(97)00311-9.
[9] M. Ghasemi, M.R. Ghasemi, S.R. Mousavi, Studying the fracture parameters and size effect of steel fiber-reinforced self-compacting concrete, Constr. Build. Mater. 201 (2019) 447–460, https://doi.org/10.1016/j.conbuildmat.2018.12.172.
[10] J. Fládr, P. Bílý, Specimen size effect on compressive and flexural strength of high-strength fibre-reinforced concrete containing coarse aggregate, Compos B Eng. 138 (2018) 77–86, https://doi.org/10.1016/j.compositesb.2017.11.032.
[11] D.Y. Yoo, N. Banthia, S.T. Kang, Y.S. Yoon, Size effect in ultra-high-performance concrete beams, Eng. Fract. Mech. 157 (2016) 86–106, https://doi.org/10.1016/j.engfracmech.2016.02.009.
[12] D.Y. Yoo, N. Banthia, J.M. Yang, Y.S. Yoon, Size effect in normal- and high-strength amorphous metallic and steel fiber reinforced concrete beams, Constr. Build. Mater. 121 (2016) 676–685, https://doi.org/10.1016/j.conbuildmat.2016.06.040.
[13] D.L. Nguyen, D.J. Kim, G.S. Ryu, K.T. Koh, Size effect on flexural behavior of ultra-high-performance hybrid fiber-reinforced concrete, Compos B Eng. 45 (2013) 1104–1116, https://doi.org/10.1016/j.compositesb.2012.07.012.
[14] S. Mindess, F.V. Lawrence, C.E. Kesler, The J-integral as a fracture criterion for fiber reinforced concrete, Cem. Concr. Res 7 (1977) 731–742, https://doi.org/10.1016/0008-8846(77)90057-6.
[15] A. Carpinteri, R. Massabó, Continuous vs discontinuous bridged-crack model for fiber-reinforced materials in flexure, Int J. Solids Struct. 34 (1997) 2321–2338, https://doi.org/10.1016/s0020-7683(96)00129-1.
[16] K. Visalvanich, A.E. Naaman, Fracture model for fiber reinforced concrete, Acids J. Proc. 80 (1983), https://doi.org/10.14359/10712.
[17] J.L. Le, Z.P. Bažant, Unified nano-mechanics based probabilistic theory of quasibrittle and brittle structures: II. Fatigue crack growth, lifetime and scaling, J. Mech. Phys. Solids 59 (2011) 1322–1337, https://doi.org/10.1016/j.jmps.2011.03.007.
[18] J. Zhang, V.C. Li, H. Stang, Size effect on fatigue in bending of concrete, J. Mater. Civ. Eng. 13 (2001) 446–453, https://doi.org/10.1061/(ASCE)0899-1561(2001)13:6(446).
[19] Z.P. Bažant, K. Xu, Size effect in fatigue fracture of concrete, Acids Mater. J. 88 (1991) 390–399.
[20] A. Carpinteri, A. Spagnoli, A fractal analysis of size effect on fatigue crack growth, Int J. Fatigue 26 (2004) 125–133, https://doi.org/10.1016/S0142-1123(03)00142-7.
[21] S. Ray, J.M. Chandra Kishen, Fatigue crack propagation model and size effect in concrete using dimensional analysis, Mech. Mater. 43 (2011) 75–86, https://doi.org/10.1016/j.mechmat.2010.12.002.
[22] N.A. Brake, K. Chatti, Prediction of size effect and non-linear crack growth in plain concrete under fatigue loading, Eng. Fract. Mech. 109 (2013) 169–185, https://doi.org/10.1016/j.engfracmech.2013.06.004.
[23] K. Kirane, Z.P. Bažant, Size effect in Paris law and fatigue lifetimes for quasibrittle materials: Modified theory, experiments and micro-modeling, Int J. Fatigue 83 (2016) 209–220, https://doi.org/10.1016/j.ijfatigue.2015.10.015.
[24] A. Carpinteri, F. Accornero, The Bridged Crack Model with multiple fibers: Local instabilities, scale effects, plastic shake-down, and hysteresis, Theor. Appl. Fract. Mech. 104 (2019), 102351, https://doi.org/10.1016/j.tafmec.2019.102351.
[25] D.C. González, Á. Mena, G. Ruiz, J.J. Ortega, E. Poveda, J. Mínguez, R. Yu, Á. De La Rosa, M.Á. Vicente, Size effect of steel fiber–reinforced concrete cylinders under compressive fatigue loading: Influence of the mesostructure, Int J. Fatigue 167 (2023), 107353, https://doi.org/10.1016/j.ijfatigue.2022.107353.
[26] J.J. Ortega, G. Ruiz, E. Poveda, D.C. González, M. Tarifa, X.X. Zhang, R.C. Yu, M.Á. Vicente, Á. de la Rosa, L. Garijo, Size effect on the compressive fatigue of fibre-reinforced concrete, Constr. Build. Mater. 322 (2022), 126238, https://doi.org/10.1016/j.conbuildmat.2021.126238.
[27] S.E.D.F. Taher, T.M. Fawzy, Performance of very-high-strength concrete subjected to short-term repeated loading, Mag. Concr. Res. 52 (2000) 219–223, https://doi.org/10.1680/macr.2000.52.3.219.
[28] S. Sinaie, A. Heidarpour, X.L. Zhao, J.G. Sanjayan, Effect of size on the response of cylindrical concrete samples under cyclic loading, Constr. Build. Mater. 84 (2015) 399–408, https://doi.org/10.1016/j.conbuildmat.2015.03.076.
[29] A. Mena-Alonso, Flexural fatigue of high-strength plain and fiber-reinforced concrete: Influence of mesostructure and study of size effect, [Dr. Thesis], Univ. Burgos (2023), https://doi.org/10.36443/10259/7855.
[30] UNE-EN 12350–8. Ensayos de hormigón fresco. Parte 8: Hormigón autocompactante. Ensayo del escurrimiento, 2011.
[31] Boletín Oficial del Estado (BOE) n.o 190, Real Decreto 470/2021, de 29 de junio, por el que se aprueba el Código Estructural, 2021.
[32] UNE-EN-12390–3. Ensayos de hormigón endurecido. Parte 3: Determinación de la resistencia a compresión de probetas, 2020.
[33] J. Yang, B. Chen, C. Nuti, Influence of steel fiber on compressive properties of ultra-high performance fiber-reinforced concrete, Constr. Build. Mater. 302 (2021), https://doi.org/10.1016/j.conbuildmat.2021.124104.
[34] M. Gesoglu, E. Güneyisi, G.F. Muhyaddin, D.S. Asaad, Strain hardening ultra-high performance fiber reinforced cementitious composites: Effect of fiber type and concentration, Compos B Eng. 103 (2016) 74–83, https://doi.org/10.1016/j.compositesb.2016.08.004.
[35] UNE-EN 12390–13. Ensayos de hormigón endurecido. Parte 13: Determinación del módulo secante de elasticidad en compresión, 2014.
[36] International Federation for Structural Concrete (fib), Model Code 2010, 2012.
[37] S.P. Singh, S.K. Kaushik, Fatigue strength of steel fibre reinforced concrete in flexure, Cem. Concr. Compos 25 (2003) 779–786, https://doi.org/10.1016/S0958-9465(02)00102-6.
[38] N.K. Banjara, K. Ramanjaneyulu, Experimental Investigations and Numerical Simulations on the Flexural Fatigue Behavior of Plain and Fiber-Reinforced Concrete, J. Mater. Civ. Eng. 30 (2018), 04018151, https://doi.org/10.1061/(asce)mt.1943-5533.0002351.
[39] D.M. Carlesso, A. de la Fuente, S.H.P. Cavalaro, Fatigue of cracked high performance fiber reinforced concrete subjected to bending, Constr. Build. Mater. 220 (2019) 444–455, https://doi.org/10.1016/j.conbuildmat.2019.06.038.
[40] F. Germano, G. Tiberti, G. Plizzari, Post-peak fatigue performance of steel fiber reinforced concrete under flexure, Mater. Struct. 49 (2016) 4229–4245, https://doi.org/10.1617/s11527-015-0783-3.
[41] D.C. González, R. Moradillo, J. Mínguez, J.A. Martínez, M.A. Vicente, Postcracking residual strengths of fiber-reinforced high-performance concrete after cyclic loading, Struct. Concr. 19 (2018) 340–351, https://doi.org/10.1002/suco.201600102.
[42] J.D. Ríos, H. Cifuentes, S. Blasón, M. López-Aenlle, A. Martínez-De La Concha, Flexural fatigue behaviour of a heated ultra-high-performance fibre-reinforced concrete, Constr. Build. Mater. 276 (2021), 122209, https://doi.org/10.1016/j.conbuildmat.2020.122209.
[43] E. Poveda, G. Ruiz, H. Cifuentes, R.C. Yu, X. Zhang, Influence of the fiber content on the compressive low-cycle fatigue behavior of self-compacting SFRC, Int J. Fatigue 101 (2017) 9–17, https://doi.org/10.1016/j.ijfatigue.2017.04.005.
[44] G.A. Plizzari, S. Cangiano, S. Alleruzzo, The fatigue behaviour of cracked concrete, Fatigue Fract. Eng. Mater. Struct. 20 (1997) 1195–1206, https://doi.org/10.1111/j.1460-2695.1997.tb00323.x.
[45] G. Gebuhr, S. Anders, M. Pise, M. Sahril, D. Brands, J. Schröder, Deterioration development of steel fibre reinforced high performance concrete in low-cycle fatigue. Advances in Engineering Materials, Structures and Systems: Innovations, Mechanics and Applications, CRC Press,, 2019, pp. 1444–1449, https://doi.org/10.1201/9780429426506-249.
[46] P.R. Sparks, J.B. Menzies, The effect of rate of loading upon the static and fatigue strengths of plain concrete in compression, Mag. Concr. Res. 25 (1973) 73–80, https://doi.org/10.1680/macr.1973.25.83.73.